Long-Term Effects on Retinal Structure and Function in a Mouse Endothelin-1 Model of Retinal Ganglion Cell Degeneration

Yamunadevi Lakshmanan,[1] Francisca Siu Yin Wong,[1] and Henry Ho-Lung Chan[1–4]

[1]Centre for Eye and Vision Research (CEVR), Hong Kong, Hong Kong
[2]Laboratory of Experimental Optometry (Neuroscience), School of Optometry, The Hong Kong Polytechnic University, Hong Kong SAR, China
[3]Research Centre for SHARP Vision (RCSV), The Hong Kong Polytechnic University, Hong Kong SAR, China
[4]University Research Facilities in Behavioral and Systems Neuroscience (UBSN), The Hong Kong Polytechnic University, Hong Kong SAR, China

Correspondence: Henry Ho-Lung Chan, School of Optometry, The Hong Kong Polytechnic University, 11 Yuk Choi Road, Hung Hom, Kowloon, Hong Kong SAR, China; henryhl.chan@polyu.edu.hk.

Received: April 18, 2023
Accepted: July 22, 2023
Published: August 10, 2023

Citation: Lakshmanan Y, Wong FSY, Chan HHL. Long-term effects on retinal structure and function in a mouse endothelin-1 model of retinal ganglion cell degeneration. *Invest Ophthalmol Vis Sci*. 2023;64(11):15. https://doi.org/10.1167/iovs.64.11.15

Purpose. To study the long-term effects of endothelin-1 (ET-1)–induced retinal pathologies in mouse, using clinically relevant tools.

Methods. Adult C57BL/6 mice (7–9 weeks old) were intravitreally injected with PBS (n = 10) or 0.25 (n = 8), 0.5 (n = 8), or 1 nmol ET-1 (n = 9) and examined using electroretinogram, optical coherence tomography (OCT), and Doppler OCT at baseline and postinjection days 10, 28, and 56. Retinal ganglion cell (RGC) survival in retinal whole mount was quantified at days 28 and 56.

Results. ET-1 induced immediate retinal arterial constriction. The significantly reduced total blood flow and positive scotopic threshold response in the 0.5- and 1-nmol ET-1 groups at day 10 were recovered at day 28. A-wave magnitude was also significantly reduced at days 10 and 28. While a comparable and significant reduction in retinal nerve fiber layer thickness was detected in all ET-1 groups at day 56, the 1-nmol group was the earliest to develop such change at day 28. All ET-1 groups showed a transient inner retinal layer thinning at days 10 and 28 and a plateaued outer layer thickness at days 10 to 56. The 1-nmol group showed a significant RGC loss over all retinal locations examined at day 28 as compared with PBS control. As for the lower-dosage groups, significant RGC density loss at central and midperipheral retina was detected at day 56 when compared with day 28.

Conclusions. ET-1 injection in mice resulted in a transient vascular constriction and reduction in retinal functions, as well as a gradual loss of retinal nerve fiber layer and RGC in a dose-dependent manner.

Keywords: endothelin-1, mice model, electroretinogram, OCT, doppler flow

A compromised blood flow to the eye due to increased IOP and/or secondary to vascular dysregulation (low perfusion pressure and other vasospasm disorders) may lead to an insufficient supply of oxygen and essential nutrients to the tissues, thereby triggering a cascade of downstream events that cause retinal ganglion cell (RGC) death.[1–5] Ocular endothelin-1 (ET-1) is an important peptide that modulates retinal blood flow and neuronal functions and is suggested to play a role in the pathophysiology of glaucoma.[6–8] ET-1 exerts its vasoactive[9] and neuroactive functions[10] through its G-protein-coupled receptors, endothelin receptor A (ET-A) and endothelin receptor B (ET-B), respectively, which are abundantly present in many ocular tissues.[11–14] Elevated levels of ET-1 in plasma,[15–24] in aqueous humor,[18,25–28] or under simulated cold vasospasm conditions[29,30] have been reported in patients with normal-tension or open-angle glaucoma. Increased expression of ET-1 receptors has also been found in postmortem glaucomatous eyes.[31] Similar results are also observed in animal models of spontaneous glaucoma[32,33] or in experimentally induced ocular hypertension.[34] Furthermore, transgenic mice with endothelial ET-1 (TET-1 mice) overexpression showed a progressive thinning in retinal nerve fiber layer, inner and outer nuclear layers, and RGC and axonal loss, along with alterations in the microvasculature.[35] Interestingly, no RGC loss was detected in ET-B–deficient rats[36] or wild-type rats treated with a dual ET-A/ET-B antagonist[37] in a Morrison's model of chronic IOP elevation. This suggests that the ET-1 and its receptors perhaps play a crucial role in RGC degeneration under conditions of elevated IOP stress and/or vascular dysregulation. Besides this, the direct effects of ET-1 on RGC survival were studied in various species such as cat,[38] rabbit,[39,40] monkey,[41–43] and rodent[44–55] by chronic application of ET-1 to the retrobulbar optic nerve, supplied via osmotic minipumps, or through an acute administration of ET-1 as a single dose of intravitreal injections. ET-1 administration in rodent eyes caused transient narrowing in retinal blood vessels[50,55] associated with the reduced blood flow,[45] blockade in axonal transport,[44,49] and decreased expression of key mitochondrial proteins,[56] resulting in increased caspase 3 activation[51,53] and loss of RGC and its axons.[45–48,50–54] As most of these changes overlap with the glaucoma disease, ET-1 models of RGC injury are used to study the molecular signaling pathways involved in RGC loss[51,52] and to evaluate possible neuroprotective therapies that antagonize ET-1's effect.[50,57–60] Intravitreal ET-1 administration in rats demonstrated a dose–response effect on RGC survival,[45–47,50,54,57] and this was seldom reported in mice.

While previous studies shed light on the molecular mechanisms of ET-1 on RGCs, there is still a lack of evidence on the longitudinal effects of ET-1 on retinal structure and functions using clinical modalities and techniques. This makes the interpretation of preclinical results and cross-comparisons with clinical data challenging. Clinically, spectral-domain optical coherence tomography (SD-OCT) is often applied to monitor changes in retinal structure by measurements of retinal layers thicknesses in patients with glaucoma,[61,62] and this has been successfully adapted in preclinical research.[63–65] For functional assessment, perimetry is the most common technique to quantify changes in the visual field sensitivity in clinical settings.[66–68] However, due to the subjective nature of this test, it is often substituted with electrophysiologic measurements of retinal cell functions in preclinical research.[65,69,70] As decreased retinal blood flow is often detected in patients with glaucoma,[71–73] Doppler OCT can be a useful tool for monitoring this change and potentially serve as one of the standard diagnostic tools in the future. Therefore, the present study reports the long-term dose–response effect of intravitreally injected ET-1 in mice retinal layer thicknesses, retinal cell functions, and retinal blood flow through applications of SD-OCT, flash electroretinogram (ERG), and Doppler OCT imaging, along with the terminal quantification of RGC survival rate using retinal whole mount.

Methods

Animals

All experimental procedures were performed according to the protocols approved by the Animal Ethics Subcommittee of The Hong Kong Polytechnic University and adhered to the ARVO Statement for the Use of Animals in Ophthalmic and Vision Research. Adult C57BL/6 mice aged between 7 and 9 weeks were housed in the animal facility at 20°C room temperature under an alternating 12-hour light/dark cycle with unrestricted food (PicoLab diet 20 (5053); PMI Nutrition International, Richmond, IN, USA) and water supply.

Experimental Design

Forty-five mice (25 males, 20 females) underwent baseline examinations of electroretinogram, optical coherence tomography (OCT), and Doppler OCT and were randomly allocated into four experimental groups: PBS, 0.25 nmol ET-1, 0.5 nmol ET-1, and 1 nmol ET-1. Intravitreal injection was performed on one randomly selected eye of each animal. To visualize the immediate effect of ET-1 in the constriction of retinal blood vessels and to examine potential postinjection intraocular complications, retinal fundus photographs were captured before and after each intravitreal injection. Follow-up examinations of ERG, OCT, and Doppler OCT were carried out at postinjection days 10, 28, and 56, after which animals were euthanized and their eyes were collected for the quantification of RGC survival. To study the interim RGC survival outcome, ∼50% of the animals in each group were euthanized earlier at day 28, while the remaining mice were euthanized at day 56 following ERG and OCT examinations.

Intravitreal Injection

Animals were first anesthetized with an intraperitoneal injection of 100 mg/kg ketamine (Alfasan International B.V., Woerden, Holland) and 20 mg/kg xylazine (Alfasan International B.V.). Briefly, a drop of short-acting topical anesthetic Provain-POS 0.5% w/v eye drops (URSAPHARM, Saarbrucken, Germany) was applied. The eyes were then dilated using Mydrin-P (Santen Pharmaceutical Co, Ltd, Osaka, Japan) that facilitated the clear view of the retina. A lubricating gel (Lacryvisc gel; Alcon, Rueil-Malmaison, France) was used to hydrate the cornea. Baseline fundus photograph was captured using Micron IV (Phoenix Research Lab, Pleasanton, CA, USA) before intravitreal injections were performed. A small incision was introduced at the conjunctiva, and the exposed sclera was punctured using a 30-gauge needle at the superotemporal limbal region. After gently pressing a clean cotton tip against the incision site for 10 seconds, intravitreal injection was carried out using a 5-µL Hamilton syringe (7633–01; Hamilton Company, NV, USA) with a blunt, 33-gauge needle. The needle was inserted at a 45-degree angle to avoid damaging the lens or the retina. Then, 2 µL PBS or ET-1 (E7764; Sigma, St. Louis, MO, USA) in PBS, at a concentration of 125, 250, or 500 µM ET-1 (i.e., 0.25, 0.5, or 1 nmol ET-1, respectively), was slowly injected into the vitreous at a rate of 1 µL/min. The needle was kept in place for about 30 seconds before it was gently and slowly removed from the injection site. Postinjection fundus photography was performed 5 minutes after the injection. Subsequently, antibiotic eyedrops (Gentamycin; Gibco, Thermo Fisher Scientific, CA, USA) were given. Animals with lens injury ($n = 3$), vitreous hemorrhage ($n = 2$), and moderate backflow while removing the injection needle ($n = 2$) and those died during follow ups ($n = 3$) were excluded from the study. For final analysis, 10 animals in PBS control, 8 each in the 0.25-nmol and 0.5-nmol ET-1 groups, and 9 in the 1-nmol ET-1 group were included.

Electroretinogram

A full-field Ganzfeld (Q450; RETI Animal, Roland Consult, Brandenburg an der Havel, Germany) with light-emitting diode (LED) light source was used to measure the differential retinal responses of retinal ganglion, bipolar, and photoreceptor cells as described previously.[65] Briefly, following an overnight dark adaptation, animals were anesthetized using ketamine (100 mg/kg) and xylazine (20 mg/kg). All procedures were conducted under a dim red light to maintain the state of dark adaptation of the animals. The pupils were dilated prior to the examination, and a drop of lubricating gel was applied to prevent corneal dehydration. The animal was placed in a warm platform that was connected to a 37°C hot water bath. For measuring the ERG, the ground and reference needle electrodes were inserted into the base of the tail and the scalp, respectively. Gold ring active electrodes (2 mm in diameter) were placed on the surface of the cornea of both eyes. Impedance was kept under 10 KΩ. First, positive scotopic threshold responses (pSTRs) were measured from light intensities ranging from −4.8 to 4.25 log cd·s/m^2 with an interstimulus interval (ISI) of 2 seconds. Thirty responses were averaged for each stimulus. This was followed by measuring scotopic responses (a- and b-waves) at an intensity of 1.3 log cd·s/m^2, with a 60-second ISI. Three responses were averaged for these stimuli. The amplitudes and implicit times of pSTRs (−4.35 log cd·s/m^2) and a- and b-wave responses were extracted for further analysis.

Optical Coherence Tomography

OCT was immediately performed after ERG to ensure that the animals were under the same anesthesia and mydriatic effects. Peripapillary retinal layers were imaged using SD-OCT (Envisu R2210; Bioptigen, Morrisville, NC, USA) with a mouse objective lens. An annular B-scan of 0.8 mm diameter (1000 A-scans) with a five-frame averaging was obtained. Later, OCT images were manually segmented to obtain the measurements of retinal nerve fiber layer thickness (RNFLT), inner retinal layer thickness (IRLT; including the inner plexiform and the inner nuclear layers), and outer retinal layer thickness (ORLT; including the outer plexiform layer and the RPE) using FIJI software (https://imagej.net/software/fiji/).

After obtaining the OCT images, retinal blood flow was evaluated using a 0.5-mm-diameter annular Doppler B-scan (1000 A scans; Envisu R2210; Bioptigen). The Doppler OCT allowed direct visualization of retinal blood flow toward (arterial; represented by red pixels) and away (venous; represented by blue pixels) from the objective. The number of red and blue pixels in the RNFLT was later quantified using a color threshold algorithm available in FIJI software (https://imagej.net/software/fiji/). First, the image with ganglion cell layer was selected and cropped. Using color thresholding, the saturation was adjusted until all the red or blue pixels in the blood vessels were included. The noise (i.e., red or blue pixels in regions other than blood vessels) was removed. Then, the number of red or blue pixels was quantified separately. This serves as indirect measurements of the retinal arterial (red pixels) and venous (blue pixels) blood flow and their vessel caliber.[74]

Immunohistochemistry in Retinal Whole Mounts

Retinal whole mounts were prepared as described previously.[75] In brief, after sacrificing the animals with CO_2 asphyxiation, eyes were collected using curved forceps and fixed with 4% paraformaldehyde (PFA) at 4°C for 20 minutes. After the excision of the cornea, lens, sclera, and vitreous, the retinas were isolated, and four incisions were made two-thirds of the way from the periphery to the optic nerve and further fixed with 4% PFA for 20 minutes. Samples were washed in PBS and blocked (blocking buffer: 10% normal goat serum [NGS], 1% bovine serum albumin [BSA], 0.05% sodium azide, and 0.5% Triton X-100 in PBS) for 1 hour at room temperature with shaking. After rinsing with PBS, the samples were incubated with primary antibodies against RBPMS (rabbit, 1:500; PhosphoSolutions, Aurora, CO, USA) for 5 days at 4°C. Samples were then washed and incubated in Alexa Fluor 488–conjugated, goat-anti-rabbit secondary antibodies (1:1000, ab150077; Abcam, Cambridge, MA, USA) at 4°C overnight. All antibodies were diluted in an incubation buffer (3% NGS, 1% BSA, 0.05% sodium azide, 0.5% Triton X-100 in PBS). Samples were washed, mounted onto microscope slides, and imaged using a confocal laser scanning microscope (LSM800; Carl Zeiss, Jena, Germany). For each retinal quadrant, sampling at the peripheral, midperipheral, and central regions was conducted through randomly selecting a region of 250 × 250 µm at 1/4, 2/4, and 3/4 of the distance from peripheral edge to the optic nerve head, respectively. Automated RGC counting was then performed using SimpleRGC, a FIJI plugin.[76] Finally, RGC counts at the central, midperipheral, and peripheral retina were obtained by averaging that respectively counts from each quadrant.

Analysis

A masked approach was used in all data collection and analysis procedures. Data were presented as mean ± SD. SPSS 26.0 (IBM Corp., Armonk, NY, USA) was used for data analysis. For OCT, ERG, and blood flow data, mixed-effect model analysis with Bonferroni post hoc correction was used. This allowed multiple comparisons to test the temporal dose responses across ET-1 dosages (interaction effect), within (time effect) and between (dosage effect) the four experimental groups. Relative changes in OCT and ERG data were defined as the percentage change from baseline. Mixed-model ANOVA with Bonferroni post hoc correction was used to test the difference in RGC counts between the four experimental groups and within groups at days 28 and 56.

Results

Effect of ET-1 on Mouse Retinal Vasculature and Ocular Blood Flow

Intravitreal injection of ET-1 led to arterial constriction in the mouse retina and a pupillary constriction. Figure 1 shows the representative fundus images of each experimental group captured at baseline and 5 minutes after intravitreal injection. While the PBS control did not cause visible changes in the retinal blood vessels (black arrowheads in Fig. 1), all three dosages of ET-1 (0.25, 0.5, and 1 nmol) resulted in an immediate constriction of retinal arteries (white arrowheads in Fig. 1). All three dosages of ET-1 injections caused a pupillary constriction, whereas PBS injection showed no such changes. For 1 nmol ET-1, the onset of pupillary constriction was earlier, around 5 minutes after the intravitreal injection. In other two lower dosages, it was observed later around 50 minutes after intravitreal injection. The long-term effects of ET-1 on retinal blood flow and its vessel caliber were quantified using Doppler OCT at baseline, postinjection days 10, 28, and 56 (Fig. 2). This allowed the comparison of pixel numbers quantified from arterial, venous, and total (sum of artery and venous) blood flows between the experimental groups across time.

For the number of pixels in arterial blood flow, a significant temporal difference was detected within groups (time effect: $P = 0.02$; dosage effect: $P = 0.34$; interaction effect: $P = 0.26$). At day 10, 1 nmol ET-1 ($P = 0.05$ for baseline vs. day 10; $P = 0.12$ as compared with PBS control) showed a decrease in number of pixels, followed by a return to baseline and PBS control levels from day 28 onward. Although not reaching statistical significance, a similar trend was observed in 0.5 nmol ET-1. On the other hand, the 0.25-nmol ET-1 group remained similar to the PBS control group throughout the experiment.

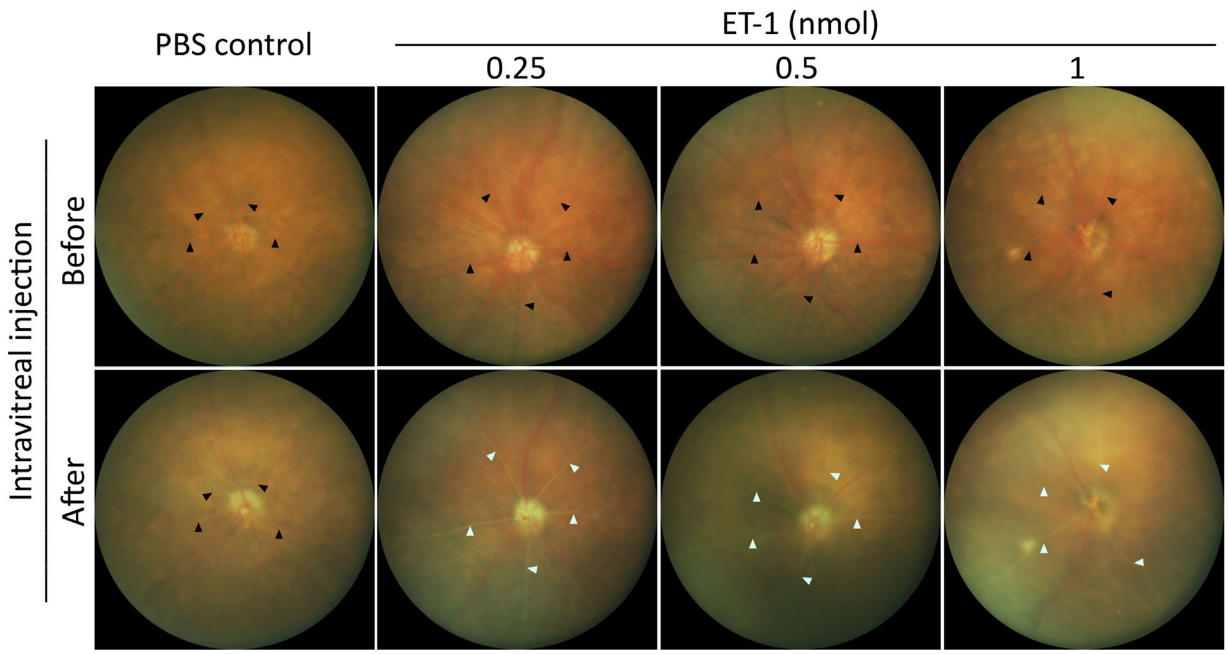

Figure 1. Fundus photographs of mouse retina captured before and after the intravitreal injection of ET-1 or PBS. PBS injection showed no visible change in the retinal blood vessels (*black arrows*). All three dosages of ET-1 (0.25, 0.5, and 1 nmol) resulted in the narrowing of retinal arteries (*white arrows*).

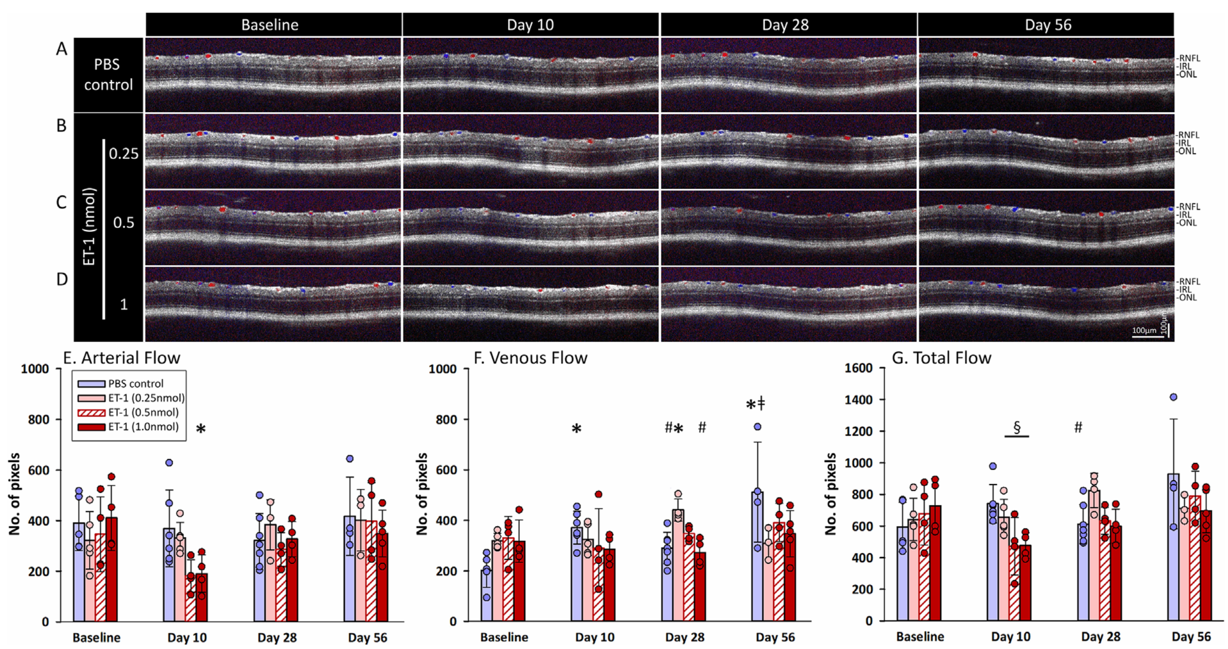

Figure 2. Long-term effects of the intravitreally injected ET-1 (0.25, 0.5, or 1 nmol) or PBS on the retinal blood flow, assessed using Doppler OCT. Annular Doppler B-scans of one representative mouse retina per group, showing the temporal changes in retinal blood flow following the intravitreal injection of (**A**) PBS or (**B–D**) 0.25, 0.5, or 1 nmol ET-1, measured at baseline and postinjection days 10, 28, and 56. Mean (**E**) arterial, (**F**) venous, and (**G**) total blood flows were compared over a period of 56 days. *Error bars*: standard deviation. Each *circle* in the *bar chart* represents an individual data point. $^{*}P < 0.05$ when compared with baseline, $^{\dagger}P < 0.05$ when compared with day 10, $^{\ddagger}P < 0.05$ when compared with day 28, $^{\S}P < 0.05$ when compared with PBS control, $^{\#}P < 0.05$ when compared with 0.25 nmol ET-1, $^{||}P < 0.05$ when compared with 0.5 nmol ET-1 using a mixed-effects model with Bonferroni post hoc test.

As for the number of pixels in venous blood flow, a significant difference was detected between the dosage groups across time (interaction effect: $P = 0.003$). All ET-1 groups showed a decreasing trend compared with the PBS control group at days 10 and 56, although they were not significant. However, at day 28, the number of pixels in the 0.25-nmol ET-1 group became significantly greater than the PBS control ($P = 0.001$) and the

1-nmol ET-1 (P = 0.001) groups as well as its baseline (P = 0.01).

The difference in number of pixels in total blood flow was significant between dosage groups across time (interaction effect: P = 0.04). Both 0.5-nmol (P = 0.04) and 1-nmol (P = 0.05) ET-1 groups were significantly lower than the PBS control group at day 10, followed by an improvement to baseline and PBS control levels from day 28 onward. At day 28, the 0.25-nmol ET-1 group showed a transient increase in number of pixels when compared with the PBS control (P = 0.04) and the 1-nmol ET-1 (P = 0.06) groups.

Dose Effect of ET-1 on Retinal Layer Thicknesses

All four measurement of retinal layers, RNFLT, IRLT, ORLT, and total retinal thickness (TRT), showed a significant difference between the experimental groups over time (interaction effect: P = 0.001, 0.01, 0.04, and 0.01, respectively). Representative OCT scan images (Figs. 3A–D), retinal layer thickness measurements (Figs. 3E–H), and their corresponding percentage change from baseline (Figs. 3I–L) are presented in Figure 3. For RNFLT (Fig. 3I), 1 nmol ET-1 was the first group to show a significant thinning at day 28 (−13.6% ± 7.2% from baseline, P = 0.01 as compared with PBS control, 0.25-nmol, and 0.5-nmol ET-1 groups) that further declined at day 56 (−16.8% ± 5.9% from baseline; P = 0.01 for day 56 vs. baseline, day 10; P = 0.02 as compared with PBS control). At the end of the study (i.e., day 56), a similar degree of thinning was also observed in the 0.25-nmol (−16.9% ± 3.8% from baseline, P = 0.03 as compared with PBS control) and 0.5-nmol (−15.6% ± 10.3% from baseline, P = 0.01 as compared with PBS control) ET-1 groups. Interestingly, while the RNFLT of the PBS control group remained stable up to day 28, a significant increase was detected at day 56 (19.1% ± 6.1% from baseline, P = 0.04 for baseline vs. day 56).

For IRLT (Fig. 3J), all ET-1 groups showed a transient thinning at days 10 and 28, followed by a recovery to baseline and PBS control group levels at day 56. On the other hand, the IRLT of the PBS control group remained stable throughout the experiment (day 56: −0.4% ± 3.7% from baseline). For ORLT and TRT thicknesses (Figs. 3K, 3L), thinning was observed in both 0.5- and 1-nmol ET-1 groups at day 10 (for 0.5 nmol ET-1, ORLT: −11% ± 7.3% from baseline, P = 0.001 for baseline vs. day 10, P = 0.003 as compared with PBS control; TRT: −9.1% ± 5.1% from baseline, P = 0.001 for baseline vs. day 10, P = 0.001 as compared with PBS control; for 1 nmol ET-1, ORLT: −8.3± 6.4% from baseline, P = 0.001 for baseline vs. day 10, TRT: −6.7% ± 4.4%, P = 0.001 for baseline vs. day 10, P = 0.03 as compared with PBS control), which was maintained up to day 56. While the thicknesses of ORLT and TRT in the PBS control group remained stable, they were slightly thinned in the lowest ET-1 dosage group, 0.25 nmol, at days 10 (ORLT: −5.1% ± 6.6% from baseline; TRT: −4.2% ± 4.8% from baseline, P = 0.05 for baseline vs. day 10, P = 0.04 as compared with PBS control) and 56 (ORLT: −8.3% ± 5.5% from baseline; TRT: −6.1% ± 4.4% from baseline).

Dose Response of ET-1 on ERG-Measured Retinal Cell Functions

The mean ERG traces of pSTRs (Fig. 4A) and scotopic responses (Fig. 4B), the amplitudes of pSTRs, scotopic b- and a-waves (Figs. 4C, 4F, 4I) and their corresponding percentage change from baseline (Figs. 4D, 4G, 4J), and the implicit times (Figs. 4E, 4H, 4K) of each experimental group are presented in Figure 4. The pSTR response varied significantly between the dosage groups with time (interaction effect: P = 0.04). On the other hand, a significant temporal change in both scotopic b- and a-waves (time effect: P = 0.01) was detected. The pSTR response of the PBS control group remained stable throughout the study, whereas that of the 1-nmol ET-1 group was significantly reduced at day 10 (PBS control: 44.4 ± 9.0 µV, 1 nmol ET-1: 30.0 ± 8.1 µV; P = 0.002 for baseline vs. day 10, P = 0.001 as compared with PBS control). The other two ET-1 groups, 0.25 nmol (31.5 ± 12.7µV; P = 0.11, as compared with PBS control) and 0.5 nmol ET-1 (22.7 ± 11.9 µV; P = 0.01 for baseline vs. day 10; P = 0.06 as compared with PBS control), also showed a reduction at day 10. On day 28, the pSTR responses were significantly recovered in both 0.25-nmol (49.9 ± 14.9 µV, P = 0.03 for days 10 vs. 28) and 0.5-nmol ET-1 groups (49.0 ± 15.0 µV, P = 0.02 for days 10 vs. 28) and remained stable up to day 56. For the 1-nmol ET-1 group, a mild improvement was shown at day 28 (38.0 ± 17.4 µV, P = 0.07 for baseline vs. day 28), and a significant recovery to the baseline and PBS control levels was observed at day 56 (1 nmol ET-1: 44.4 ± 18.9 µV, P = 0.01 for days 10 vs. 56).

For scotopic b-wave responses, the amplitudes were moderately reduced in 1 nmol ET-1 at days 10 and 28 (day 10: 379.4 ± 119 µV; day 28: 382.5 ± 137.0 µV, P = 0.08 for baseline vs. days 10, 28). Similarly, 0.5 nmol ET-1 showed reduced responses at days 10 (418.3 ± 96.7 µV, P = 0.05), 28 (401 ± 79.5 µV, P = 0.10), and 56 (368.8 ± 115.0 µV, P = 0.04) as compared with its baseline. Although the reduction in the 0.25-nmol ET-1 group at day 10 did not reach statistical significance (baseline: 405 ± 82.2 µV; day 10: 326.1 ± 113.7 µV), improvement in the amplitude to baseline levels was observed at day 56 (422.5 ± 65 µV). The a-wave amplitudes of the 0.5-nmol (day 10: 193.2 ± 27.1 µV; day 28: 234.4 ± 70.5 µV) and 1-nmol (day 10: 201.2 ± 45.5 µV; day 28: 203.9 ± 58.3) ET-1 groups were reduced significantly at both days 10 (P = 0.01) and 28 (P = 0.02) when compared with their baselines (0.5 nmol ET-1: 327.7 ± 87.3 µV; 1 nmol ET-1: 292.7 ± 61.4 µV). While the response in the 1-nmol ET-1 group showed a mild improvement at day 56 (247.4 ± 67.2 µV), that of the 0.5-nmol ET-1 group did not show any improvement (208.7 ± 52.3 µV, P = 0.01, as compared with baseline). As for the 0.25-nmol ET-1 group, a reduction was observed at day 10 (178.1 ± 50.5 µV, P = 0.11, as compared with baseline; P = 0.04, as compared with PBS control), which was later improved at day 28 (220.0 ± 50.6 µV) and further recovered to its baseline at day 56 (baseline: 249.4 ± 69.6 µV; day 56: 240.3 ± 14.1 µV). At day 56, both the scotopic b- and a-wave responses were not significantly different from PBS control.

No significant difference was detected between the pSTR implicit times of different treatment groups or time points. At day 10, the b-wave response of the 1-nmol ET-1 group was significantly delayed (P = 0.04 as compared with PBS control; P = 0.01 for baseline vs. day 10). However, it was improved later to a level comparable with the baseline from day 28. For the a-wave implicit time, an early onset of response was detected in the 0.25-nmol (P = 0.01 for baseline vs. day 56, P = 0.02 for days 10 vs. 56) and 0.5-nmol groups (P = 0.02 for baseline vs. day 56).

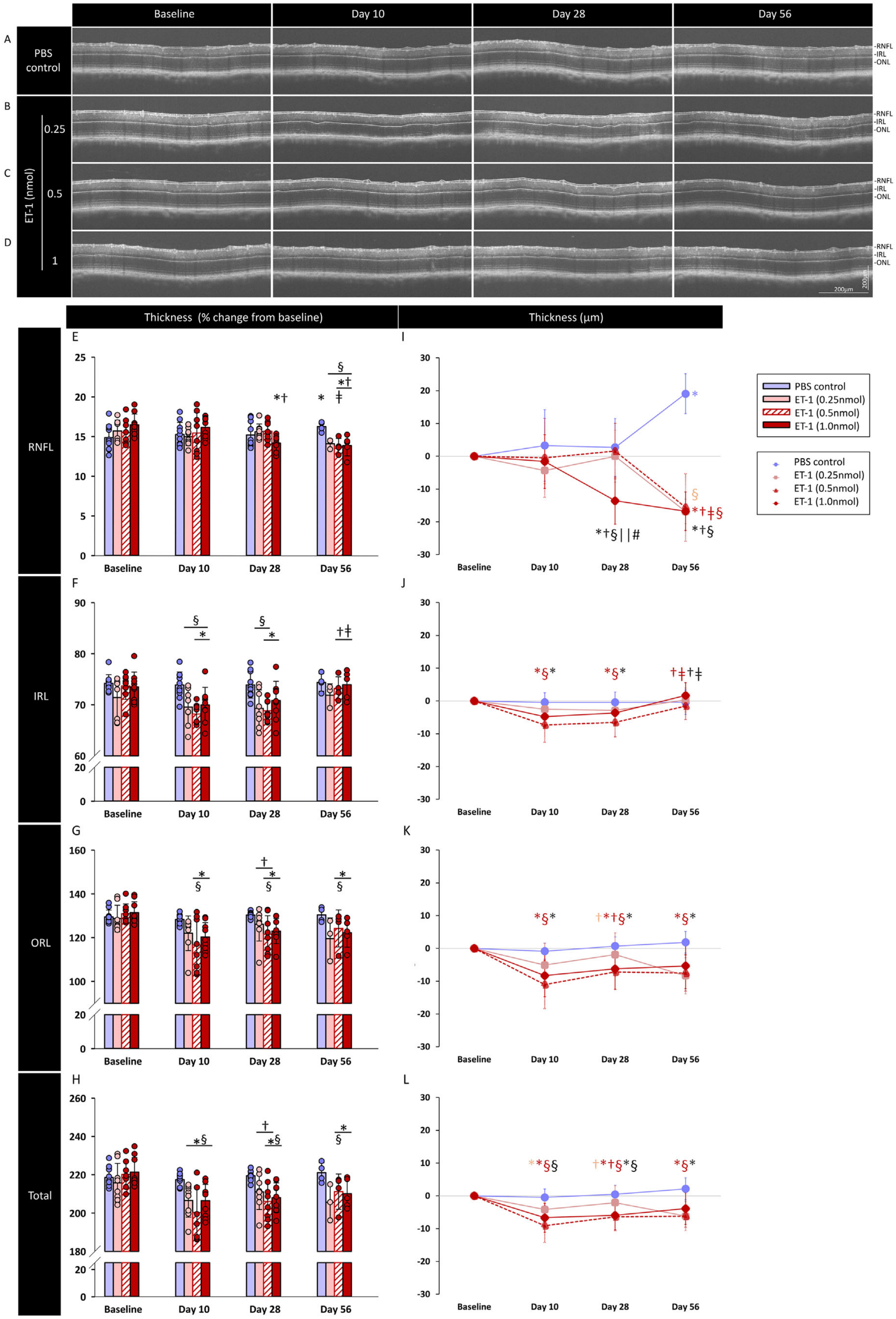

FIGURE 3. Long-term effects of intravitreally injected ET-1 (0.25, 0.5, or 1 nmol) or PBS on differential retinal layer thicknesses. The segmented SD-OCT B-scans of one representative mouse retina per group after the intravitreal injection of (**A**) PBS or (**B–D**) 0.25, 0.5, or 1 nmol ET-1

at the baseline and postinjection days 10, 28, and 56. Mean peripapillary retinal thicknesses of (**E**) RNFLT, (**F**) IRLT, (**G**) ORLT, and (**H**) total retinal thickness and (**I–L**) the corresponding percentage change from baseline were compared over a period of 56 days. *Error bars*: standard deviation. Each *circle* in the *bar chart* represents an individual data point. **P* < 0.05 when compared with baseline, †*P* < 0.05 when compared with day 10, ‡*P* < 0.05 when compared with day 28, §*P* < 0.05 when compared with PBS control, #*P* < 0.05 when compared with 0.25 nmol ET-1, ||*P* < 0.05 when compared with 0.5 nmol ET-1 using a mixed-effects model with Bonferroni post hoc test.

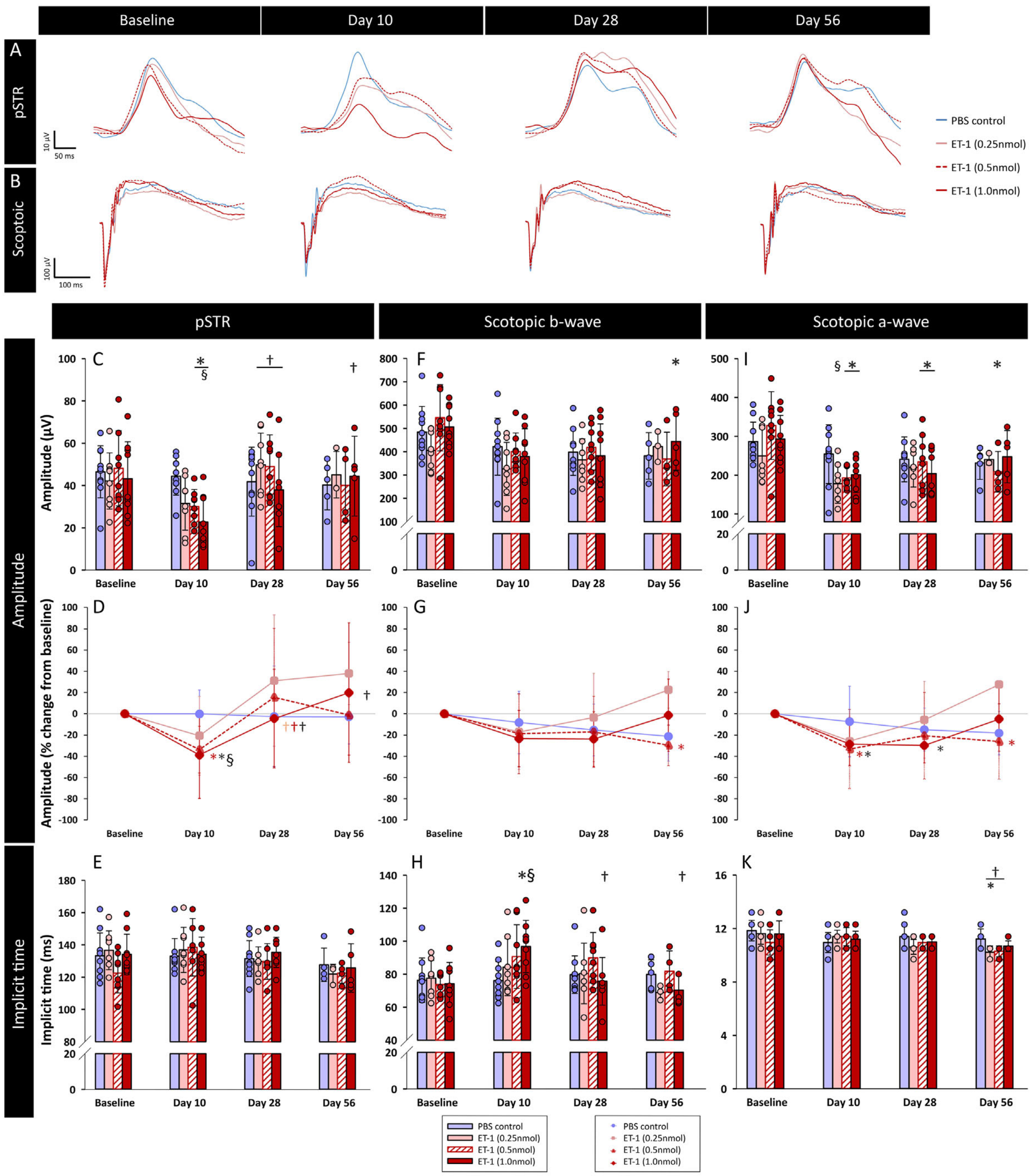

Figure 4. Long-term effects of intravitreally injected ET-1 (0.25, 0.5, or 1 nmol) or PBS on retinal functions. The averaged ERG traces of (**A**) pSTR and (**B**) scotopic responses from each experimental group measured at baseline and postinjection days 10, 28, and 56. Mean amplitudes of (**C**) pSTR, (**F**, **I**) scotopic b- and a-waves, (**D**, **G**, **J**) the corresponding percentage change from baseline, and (**E**, **H**, **K**) implicit times were compared over a period of 56 days. *Error bars*: standard deviation. Each *circle* in the *bar chart* represents an individual data point. **P* < 0.05 when compared with baseline, †*P* < 0.05 when compared with day 10, ‡*P* < 0.05 when compared with day 28, §*P* < 0.05 when compared with PBS control using a mixed-effects model with Bonferroni test.

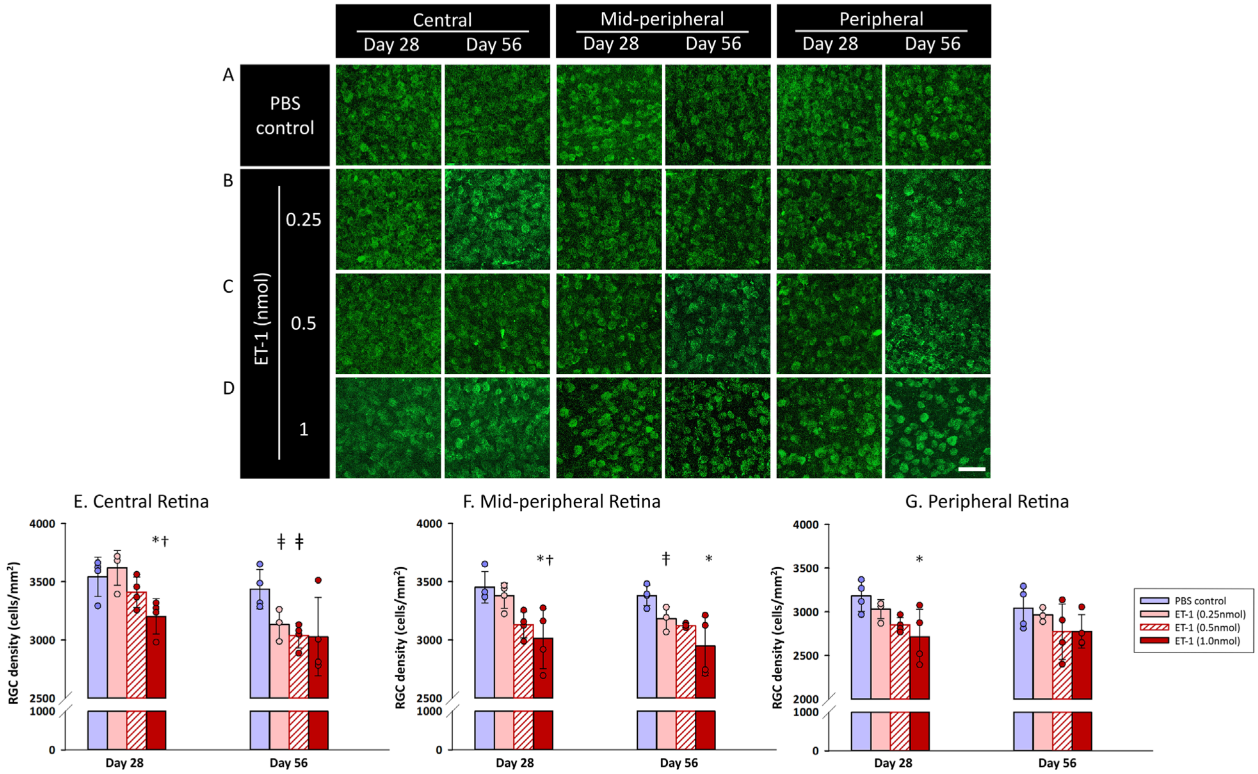

FIGURE 5. Effects of intravitreally injected ET-1 (0.25, 0.5, or 1 nmol) or PBS on RGC survival. The representative retinal flat mounts of mice receiving (**A**) PBS control or (**B**) 0.25 nmol, (**C**) 0.5 nmol, and (**D**) 1 nmol ET-1, captured at the center, midperipheral, and peripheral retinal locations at days 28 and 56. Mean RGC density from the (**E**) central, (**F**) midperipheral, and (**G**) peripheral retinal locations were compared across groups at days 28 and 56 ($n = 4$ in each group). *Error bars*: standard deviation. Each *circle* in the *bar chart* represents an individual data point. *$P < 0.05$ when compared with PBS control, †$P < 0.05$ when compared with 0.25 nmol ET-1, ‡$P < 0.05$ when compared with week 4 using a mixed-model ANOVA with Bonferroni post hoc test.

Dose Effect of ET-1 on RGC Survival

RGC survival was assessed at two time points (days 28 and 56) and at three retinal locations (central, midperipheral, and peripheral) (Fig. 5). For RGC density, a significant dosage main effect ($P = 0.01$) was detected in all three retinal locations, whereas a significant time main effect was observed in the central and midperipheral locations ($P = 0.003$ for central, $P = 0.03$ for midperipheral, and $P = 0.59$ for peripheral retina).

At day 28, the RGC densities of the 1-nmol ET-1 group were significantly reduced in all three retinal locations (central: $P = 0.05$, as compared with PBS control and 0.25 nmol ET-1; midperipheral: $P = 0.02$, as compared with PBS control and peripheral: $P = 0.04$, as compared with PBS control). At day 56, a significant reduction was detected only at the midperipheral retinal location of the 1-nmol ET-1 group ($P = 0.01$, as compared with PBS control). As for the lower-dosage groups, significant reductions in RGC densities were observed at the central ($P = 0.02$ for 0.25 nmol and 0.5 nmol ET-1) and midperipheral retina ($P = 0.04$ for 0.25 nmol ET-1) at day 56 when compared with day 28. The RGC density showed a moderate correlation with relative percentage change in RNFLT (Supplementary Fig. S1).

DISCUSSION

The present study reports the long-term dose–response effects of ET-1 on retinal blood flow, retinal layer thicknesses, retinal cell responses, and RGC survival. Intravitreal injection of ET-1 caused an immediate constriction of retinal arteries and a reduction in the number of pixels in Doppler flow. The reduction in blood flow occurred in a dose-dependent manner such that the higher dosages led to prolonged recovery from vasoconstriction. Similarly, for retinal cell function, a transient reduction in ganglion and photoreceptor cell responses was detected. As the response of second-order neurons (i.e., b-wave) was not significantly affected by the decrease in photoreceptor cell function (i.e., a-wave), it suggested that the reduction in RGC function was likely independent of the photoreceptor response. Subsequently, a loss in RNFL and RGC was observed as early as day 28 in the highest dosage group (1 nmol ET-1), while these changes were developed later at day 56 in the other two lower-dosage groups (0.25 nmol and 0.5 nmol ET-1).

Glaucoma is a complex disease caused by raised IOP, vascular dysregulation, and/or several IOP-independent factors. In recent years, there is growing evidence indicating the potential role of ET-1 in RGC neurodegeneration.[6–8] Animal models of ET-1 have been used to examine its effects on retinal neurons,[44–55] study the potential pathways involved in RGC degeneration,[51,52] and explore the potential treatment options combating its effects.[50,57–60] This was generally approached by studying the dose–response effect of ET-1 and then choosing an appropriate dosage that results in substantial RGC loss for further investigations. Earlier studies reported the dose–response effect of intravitreally injected ET-1 on axonal transport[44] and RGC survival[46] in rats. With regard to axonal transport, 2 nmol ET-1 (i.e., 4 μL of 500 μM ET-1) was shown to significantly affect the anterograde axonal transport as compared with 0.3 and 0.4 nmol ET-1 in Sprague-Dawley rats.[44] Subsequently, a similar dosage of 2.5 nmol ET-1 resulted in a 25% loss in RGC after 2 weeks of injection, whereas the dosages of 0.025 and 0.25 nmol ET-1 did not show such loss.[46] Another dose–response study (0.2–200 pmol ET-1) showed that a dosage of 20 pmol was sufficient to induce 43% loss in RGC.[50] In the same study, the fluorogold labeling of RGC was performed 3 weeks after ET-1 injection. As ET-1 is known to affect the retrograde axonal transport and recovery to normalize axonal transport takes a longer time, the applied fluorogold would label not only dead RGCs but also functional RGCs with impaired axonal flow, leading to a potential overestimation of RGC loss. Although there was no literature evidence on the dose response of ET-1 in mice, few studies have shown that 1 nmol ET-1 (i.e., 2 μL of 500 μM concentration) was sufficient to cause RGC loss in mice.[51,52] This is comparable to the effective concentrations of ET-1 (500 μM) reported earlier in rats. Therefore, in the present study, the long-term dose–response effects of 0.25, 0.5, and 1 nmol ET-1 (equivalent to 125, 250, and 500 μM ET-1 concentration per μL, respectively) on retinal structure and function were studied.

Intravitreal ET-1 injection in mice induced constriction in the retinal arteries (Fig. 1), which was also indicated by reduction in number of pixels in the arterial flow. A previous study showed that intravitreal injection of 1 nmol ET-1 caused 3 hours of vasoconstriction, which took at least 6 hours to restore normal perfusion and was sufficient to induce retinal hypoxia in RGCs/Müller glia for 24 hours.[51] Although the present study did not monitor how long the effects of vasoconstriction lasted in each dosage of ET-1, the restoration of retinal flow was evaluated using Doppler imaging. Our findings indicated that the time to full retinal reperfusion following ET-1 injection was dose dependent, with retinas receiving higher doses of ET-1 taking longer to achieve full recovery in the blood flow and thereby being exposed to longer periods of vasoconstriction and hypoxia. While this calls into question whether a single dose of ET-1 can exhibit such a long-term effect on vascular regulation, reports from previous studies suggested this possibility. A brief application of ET-1 on the surface of the rat optic nerve caused a 68% reduction in blood flow[45] and transiently blocked the retrograde axonal flow for at least 2 hours with a complete recovery in 6 hours.[49] On the other hand, an intravitreal injection of 2 nmol ET-1 in rats causing vasoconstriction of retinal vessels was enough to affect the anterograde axonal transport for at least 21 days.[44] Therefore, intravitreal dosing of ET-1 potentially causes vasoconstriction for extended durations, thereby affecting the retinal circulation and axonal transport in a dose-dependent manner and hence impeding the proper functioning of RGCs and their survival.

The current study showed that ET-1–induced vasoconstriction affected all three retinal layers. While ORLT thinning was sustained, IRLT thinning was reversed at the end of the study for all three dosage groups. It should be highlighted that the OCT retinal thickness measurements can be impacted by changes in retinal neurons as well as the constriction of vascular plexus, which is embedded in different retinal layers. This includes the superficial vascular plexus in the RNFL and the intermediate and deep vascular plexus in the inner and outer plexiform layers of the retina, respectively. Therefore, the initial reduction in IRL from days 10 to 28 and subsequent recovery at day 56 could potentially be attributed to the prolonged effect of vasoconstriction, followed by the restoration to normal vessel caliber over the course of the study.

We have detected degenerative outer retinal changes that were nonprogressive in the ET-1–injected eyes. A previous study on TET-1 mice, which overexpresses ET-1, also reported significant thinning in the outer nuclear layer, along with the inner layers.[35] Among the layers taken into account for OCT-based ORLT measurements, which includes the outer plexiform, outer nuclear, photoreceptors segments, and RPE layers, the outer plexiform layer is the only layer embedded with the deep vascular plexus. The rest of the outer retina depends on the choroid for nutrient supply and material exchange through diffusion. This implied that the impact of ET-1–induced changes in the vascular plexus on the ORLT measurements is limited. This also suggested other mechanisms may be involved in the nonprogressive thinning of ORLT detected. Since ET-1 receptors are present in both the outer retina and the choroidal vessels,[11,77] it is possible that outer retinal degeneration is a result of ET-1–mediated neuronal changes and/or a transient nutrient deficiency from choroidal supply. Further investigation is needed to understand the mechanisms involved in ET-1–mediated outer retinal changes. Interestingly, the dose–response effect of ET-1 was clearly observed in the rate of RNFL loss. It is possible that the higher ET-1 dosage accelerated the rate of degeneration and resulted in earlier RNFL thinning, as seen at day 28, whereas lower dosages caused a slower rate of degeneration, and thus the effects became observable later at day 56. However, further investigation on the temporal course of events, such as JUN or caspase 3 activation as reported earlier,[51] leading to neuronal loss in various dosages, is required. A previous study on ET-1–injected rats reported a similar trend, in which IRLT and TRT were the first to show thinning at week 1, followed by RNFL at week 2.[50] While the higher dosages of ET-1 (20, 60, and 200 pmol) led to a significant RNFL loss, lower dosages (2 and 5 pmol ET-1) showed a declining trend at the end of the second week. However, the relatively short follow-up period used in these studies was unable to show whether the RNFL thinning at lower dosages was progressive at later time points, as observed in the present study. It is worthwhile to mention that for the PBS control group, the RNFLT showed an increase at day 56 while the inner and outer retina thicknesses remained unchanged. We speculated that this may be an effect of the raised venous and total blood flow at day 56 or due to animal variability.

RGC survival was also impacted by ET-1–induced constriction in a similar fashion in the present study. The 1-nmol ET-1 group was the first to show an RGC loss, followed by other two lower-dosage groups. The RGC density was significantly and positively associated with RNFLT (Supplementary Fig. S1). The association was greater at the central retina ($r = 0.56$), followed by the midperipheral ($r = 0.46$) and the peripheral ($r = 0.43$) regions. This corroborated with the OCT retinal thickness measurements that were taken from the peripapillary region, which correlated with the central retina used in RGC quantification. However, the observed RGC loss was of a lower magnitude when compared to previous studies that reported 26% RGC loss using 1 nmol ET-1 in mice.[55] This could be due to a smaller sample size as half of the animals were euthanized at each time point (i.e., at days 28 and 56) for the investigation of long-term RGC loss. Interestingly, one study reported that ET-1 caused a significant, region-specific RGC loss at the midperipheral and peripheral retina.[52] Alternatively, some studies detected a greater RGC loss at the central region,[60] while others reported a uniform loss across all retinal regions.[45] However, in the present study, we observed distinct findings at different time points. At day 28, the loss in RGC density was greatest at the peripheral retinal region, followed by the midperipheral and central retina. However, at day 56, this trend was reversed, with RGC loss from the central and midperipheral retina greater than the peripheral region. These findings suggested that the intravitreal injection of ET-1 caused a gradual loss in RGC, starting from the peripheral retinal region, and slowly progressing toward the central region with time.

In regard to retinal cell functions, all three dosages of ET-1 caused a transient reduction in ganglion (pSTR) and photoreceptor (a-wave) functions with maximum reduction in pSTR (∼40%) observed in the 1-nmol ET-1 group. ET-1 showed minimal effect on scotopic b-wave, and the difference between the ET-1 groups was insignificant. While there are no previous reports on the long-term effects of ET-1 on electrophysiologic measurement of retinal functions, one study investigated its short-term effect. In Wistar rats, 20 pmol ET-1 significantly reduced both pattern-induced visually evoked potentials (∼70%) and pattern ERG (∼33%) after 5 days of intravitreal injection.[59] The same study also showed that the scotopic responses were unaffected. Another study demonstrated that 2.5 nmol ET-1 in rats had a prolonged effect on the pupillary responses, with the duration of light response increased by 25% and the velocity of pupillary constriction decreased by 30% at 3 weeks after intravitreal injection.[46] Collectively, these findings suggest that the lower dosages of ET-1 injection affected the retinal functions transiently, and this effect could be prolonged in higher dosages. With regard to the structure–function relationship, the restoration of pSTR responses does not conform with the structural loss (i.e., RNFL thinning) or the decrease in RGC survival observed at days 28 and 56; however, it paralleled the recovery in arterial flow. We speculate that there are two possibilities to this disparity: (a) both RNFL and inner plexiform layer (IPL) have a dense vascular plexus and are regions of high metabolic demand. The restoration in blood flow following a brief period of ET-1–induced vasoconstriction would eventually improve the retinal cell metabolism and hence the retinal electrophysiologic activities. (b) As the level of damage, in terms of RGC loss, induced in the models is relatively mild, the summated retinal responses measured by Ganzfeld ERG may not be sensitive enough or may lack the specificity required to reflect this change. Alternatively, the more sensitive pattern ERG or multifocal ERG can be applied.[78,79]

While the present study did not investigate the potential mechanisms of ET-1 involved in RGC neurodegeneration or its molecular pathways, a handful of studies have explored this previously. Increased RGC apoptosis and increased ET-B expression were reported in RGC-5 cells treated with ET-1 and rats intravitreally injected with ET-1.[48] The effects were attenuated when RGC-5 cells were cotreated with ET-B antagonist or when ET-B deficient rats were used, indicating a potential role of ET-B in RGC neurodegeneration.[48] In contrast, a recent study[53] demonstrated that the conditional deletion of ET-A, ET-B, or both ET-A/ET-B receptors from retinal neurons and microglia did not prevent the ET-1–induced vasoconstriction or caspase 3 activation in RGC. However, the deletion of ET-A receptor either from full-body or mural cells inhibited both vasoconstriction and RGC death but not the global deletion of ET-B receptor.[53] This suggested that ET-1–induced RGC death is mainly driven by vascular mural cells expressing ET-A receptors, causing vasoconstriction and subsequent neurodegeneration process. Furthermore, the 1-nmol ET-1 injection caused a JUN activation in 30% of RGC cells at day 1 and increased caspase 3 activation at day 5, which resulted in 26% RGC loss at day 28.[51] Nevertheless, the same study showed that ET-1 did not cause any damage to amacrine cells,[51] indicating that the model did not induce significant retinal ischemia. Subsequent studies also showed that the RGC loss was attenuated when ET-1 was injected in conditional knockout of c-JUN[51] or JNK2 knockout mice,[52] suggesting the involvement of the JNK-JUN signaling pathway in ET-1–induced RGC death.

The present study primarily presents the long-term dose–response effects of ET-1–induced vasoconstriction on retinal structures and functions in a mice model. The recovery from ET-1–induced arterial flow reduction (in terms of the number of pixels in Doppler flow) was affected in a dose-dependent manner. While all dosages resulted in neuronal loss (RNFL/RGC), the manifestation of such loss was earlier in the higher ET-1 dosage. This suggested that an initial period of vascular compromise was sufficient to cause neuronal loss; however, the rate of degeneration seems to be related to the dosages of ET-1. As the degenerative effects at lower dosages cannot be ascertained without performing long-term assessments, further studies on the prolonged impact of ET-1 on vascular endothelial cells and the associated molecular mechanisms involved in neuronal degeneration, including that in the outer retina, are warranted. This mouse model, with single ET-1 injection, demonstrated vasoconstriction, followed by a gradual development of RGC injury from mild to moderate, independent of IOP elevation. Its outcomes resembled certain presentations of clinical glaucoma subtypes (e.g., normal-tension glaucoma) that exhibit RGC neurodegeneration in the absence of elevated IOP. Given that the model is a minimally invasive, IOP-independent neurodegeneration that involves a slow and progressive loss in RNFL/RGC, this can potentially be applied to test neuroprotective therapeutics targeting RGCs. By monitoring the changes in the retinal structure and function using clinical tools, our findings may add to the current body of evidence on ET-1–induced RGC degeneration and facilitate the comparison between preclinical and clinical data.

Acknowledgments

Supported by the PolyU Central Research Grants (UAG1, UAHD, UALH).

Disclosure: **Y. Lakshmanan**, None; **F.S.Y. Wong**, None; **H.H.-L. Chan**, None

References

1. Osborne NN, Ugarte M, Chao M, et al. Neuroprotection in relation to retinal ischemia and relevance to glaucoma. *Surv Ophthalmol*. 1999;43(suppl 1):S102–S128.
2. Quigley HA. Neuronal death in glaucoma. *Prog Retin Eye Res*. 1999;18:39–57.
3. Tezel G, Wax MB. Hypoxia-inducible factor 1alpha in the glaucomatous retina and optic nerve head. *Arch Ophthalmol*. 2004;122:1348–1356.

4. Flammer J, Orgül S, Costa VP, et al. The impact of ocular blood flow in glaucoma. *Prog Retin Eye Res*. 2002;21:359–393.
5. Flammer J, Haefliger IO, Orgül S, Resink T. Vascular dysregulation: a principal risk factor for glaucomatous damage? *J Glaucoma*. 1999;8:212–219.
6. Yorio T, Krishnamoorthy R, Prasanna G. Endothelin: is it a contributor to glaucoma pathophysiology? *J Glaucoma*. 2002;11:259–270.
7. Good TJ, Kahook MY. The role of endothelin in the pathophysiology of glaucoma. *Expert Opin Ther Targets*. 2010;14:647–654.
8. Shoshani YZ, Harris A, Shoja MM, et al. Endothelin and its suspected role in the pathogenesis and possible treatment of glaucoma. *Curr Eye Res*. 2012;37:1–11.
9. Yanagisawa M, Kurihara H, Kimura S, et al. A novel potent vasoconstrictor peptide produced by vascular endothelial cells. *Nature*. 1988;332:411–415.
10. Shihara M, Hirooka Y, Hori N, et al. Endothelin-1 increases the neuronal activity and augments the responses to glutamate in the NTS. *Am J Physiol*. 1998;275:R658–665.
11. Chakravarthy U, Douglas AJ, Bailie JR, McKibben B, Archer DB. Immunoreactive endothelin distribution in ocular tissues. *Invest Ophthalmol Vis Sci*. 1994;35:2448–2454.
12. Ripodas A, de Juan JA, Roldán-Pallarés M, et al. Localisation of endothelin-1 mRNA expression and immunoreactivity in the retina and optic nerve from human and porcine eye. Evidence for endothelin-1 expression in astrocytes. *Brain Res*. 2001;912:137–143.
13. Fernández-Durango R, Rollín R, Mediero A, et al. Localization of endothelin-1 mRNA expression and immunoreactivity in the anterior segment of human eye: expression of ETA and ETB receptors. *Mol Vis*. 2003;9:103–109.
14. MacCumber MW, D'Anna SA. Endothelin receptor-binding subtypes in the human retina and choroid. *Arch Ophthalmol*. 1994;112:1231–1235.
15. Lommatzsch C, Rothaus K, Schopmeyer L, et al. Elevated endothelin-1 levels as risk factor for an impaired ocular blood flow measured by OCT-A in glaucoma. *Sci Rep*. 2022;12:11801.
16. Konieczka K, Terelak-Borys B, Skonieczna K, Schoetzau A, Grabska-Liberek I. Age dependence of plasma endothelin levels in glaucoma patients. *J Physiol Pharmacol*. 2020;71(6):905–910.
17. Li S, Zhang A, Cao W, Sun X. Elevated plasma endothelin-1 levels in normal tension glaucoma and primary open-angle glaucoma: a meta-analysis. *J Ophthalmol*. 2016;2016:2678017.
18. Ahoor MH, Ghorbanihaghjo A, Sorkhabi R, Kiavar A. Klotho and endothelin-1 in pseudoexfoliation syndrome and glaucoma. *J Glaucoma*. 2016;25:919–922.
19. López-Riquelme N, Villalba C, Tormo C, et al. Endothelin-1 levels and biomarkers of oxidative stress in glaucoma patients. *Int Ophthalmol*. 2015;35:527–532.
20. Cellini M, Strobbe E, Gizzi C, Balducci N, Toschi PG, Campos EC. Endothelin-1 plasma levels and vascular endothelial dysfunction in primary open angle glaucoma. *Life Sci*. 2012;91:699–702.
21. Chen HY, Chang YC, Chen WC, Lane HY. Association between plasma endothelin-1 and severity of different types of glaucoma. *J Glaucoma*. 2013;22:117–122.
22. Emre M, Orgül S, Haufschild T, Shaw SG, Flammer J. Increased plasma endothelin-1 levels in patients with progressive open angle glaucoma. *Br J Ophthalmol*. 2005;89:60–63.
23. Sugiyama T, Moriya S, Oku H, Azuma I. Association of endothelin-1 with normal tension glaucoma: clinical and fundamental studies. *Surv Ophthalmol*. 1995;39(suppl 1):S49–S56.
24. Cellini M, Possati GL, Profazio V, Sbrocca M, Caramazza N, Caramazza R. Color Doppler imaging and plasma levels of endothelin-1 in low-tension glaucoma. *Acta Ophthalmol Scand Suppl*. 1997;224:11–13.
25. Choritz L, Machert M, Thieme H. Correlation of endothelin-1 concentration in aqueous humor with intraocular pressure in primary open angle and pseudoexfoliation glaucoma. *Invest Ophthalmol Vis Sci*. 2012;53:7336–7342.
26. Koukoula SC, Katsanos A, Tentes IK, Labiris G, Kozobolis VP. Retrobulbar hemodynamics and aqueous humor levels of endothelin-1 in exfoliation syndrome and exfoliation glaucoma. *Clin Ophthalmol*. 2018;12:1199–1204.
27. Ghanem AA, Elewa AM, Arafa LF. Endothelin-1 and nitric oxide levels in patients with glaucoma. *Ophthalmic Res*. 2011;46:98–102.
28. Iwabe S, Lamas M, Vásquez Pélaez CG, Carrasco FG. Aqueous humor endothelin-1 (Et-1), vascular endothelial growth factor (VEGF) and cyclooxygenase-2 (COX-2) levels in Mexican glaucomatous patients. *Curr Eye Res*. 2010;35:287–294.
29. Terelak-Borys B, Czechowicz-Janicka K. Investigation into the vasospastic mechanisms in the pathogenesis of glaucomatous neuropathy. *Klin Oczna*. 2011;113:201–208.
30. Nicolela MT, Ferrier SN, Morrison CA, et al. Effects of cold-induced vasospasm in glaucoma: the role of endothelin-1. *Invest Ophthalmol Vis Sci*. 2003;44:2565–2572.
31. Wang L, Fortune B, Cull G, Dong J, Cioffi GA. Endothelin B receptor in human glaucoma and experimentally induced optic nerve damage. *Arch Ophthalmol*. 2006;124:717–724.
32. Källberg ME, Brooks DE, Garcia-Sanchez GA, Komàromy AM, Szabo NJ, Tian L. Endothelin 1 levels in the aqueous humor of dogs with glaucoma. *J Glaucoma*. 2002;11:105–109.
33. Källberg ME, Brooks DE, Gelatt KN, Garcia-Sanchez GA, Szabo NJ, Lambrou GN. Endothelin-1, nitric oxide, and glutamate in the normal and glaucomatous dog eye. *Vet Ophthalmol*. 2007;10(suppl 1):46–52.
34. Prasanna G, Hulet C, Desai D, et al. Effect of elevated intraocular pressure on endothelin-1 in a rat model of glaucoma. *Pharmacol Res*. 2005;51:41–50.
35. Mi XS, Zhang X, Feng Q, Lo AC, Chung SK, So KF. Progressive retinal degeneration in transgenic mice with overexpression of endothelin-1 in vascular endothelial cells. *Invest Ophthalmol Vis Sci*. 2012;53:4842–4851.
36. Minton AZ, Phatak NR, Stankowska DL, et al. Endothelin B receptors contribute to retinal ganglion cell loss in a rat model of glaucoma. *PLoS One*. 2012;7:e43199.
37. Kodati B, McGrady NR, Jefferies HB, Stankowska DL, Krishnamoorthy RR. Oral administration of a dual ET(A)/ET(B) receptor antagonist promotes neuroprotection in a rodent model of glaucoma. *Mol Vis*. 2022;28:165–177.
38. Granstam E, Wang L, Bill A. Ocular effects of endothelin-1 in the cat. *Curr Eye Res*. 1992;11:325–332.
39. Takei K, Sato T, Nonoyama T, Miyauchi T, Goto K, Hommura S. A new model of transient complete obstruction of retinal vessels induced by endothelin-1 injection into the posterior vitreous body in rabbits. *Graefes Arch Clin Exp Ophthalmol*. 1993;231:476–481.
40. Cioffi GA, Orgül S, Onda E, Bacon DR, Van Buskirk EM. An in vivo model of chronic optic nerve ischemia: the dose-dependent effects of endothelin-1 on the optic nerve microvasculature. *Curr Eye Res*. 1995;14:1147–1153.
41. Orgül S, Cioffi GA, Bacon DR, Van Buskirk EM. An endothelin-1-induced model of chronic optic nerve ischemia in rhesus monkeys. *J Glaucoma*. 1996;5:135–138.
42. Cioffi GA, Sullivan P. The effect of chronic ischemia on the primate optic nerve. *Eur J Ophthalmol*. 1999;9(suppl 1):S34–S36.

Investigative Ophthalmology & Visual Science

43. Cioffi GA, Wang L, Fortune B, et al. Chronic ischemia induces regional axonal damage in experimental primate optic neuropathy. *Arch Ophthalmol*. 2004;122:1517–1525.
44. Stokely ME, Brady ST, Yorio T. Effects of endothelin-1 on components of anterograde axonal transport in optic nerve. *Invest Ophthalmol Vis Sci*. 2002;43:3223–3230.
45. Chauhan BC, LeVatte TL, Jollimore CA, et al. Model of endothelin-1-induced chronic optic neuropathy in rat. *Invest Ophthalmol Vis Sci*. 2004;45:144–152.
46. Lau J, Dang M, Hockmann K, Ball AK. Effects of acute delivery of endothelin-1 on retinal ganglion cell loss in the rat. *Exp Eye Res*. 2006;82:132–145.
47. Taniguchi T, Shimazawa M, Sasaoka M, Shimazaki A, Hara H. Endothelin-1 impairs retrograde axonal transport and leads to axonal injury in rat optic nerve. *Curr Neurovasc Res*. 2006;3:81–88.
48. Krishnamoorthy RR, Rao VR, Dauphin R, Prasanna G, Johnson C, Yorio T. Role of the ETB receptor in retinal ganglion cell death in glaucoma. *Can J Physiol Pharmacol*. 2008;86:380–393.
49. Wang X, Baldridge WH, Chauhan BC. Acute endothelin-1 application induces reversible fast axonal transport blockade in adult rat optic nerve. *Invest Ophthalmol Vis Sci*. 2008;49:961–967.
50. Nagata A, Omachi K, Higashide T, et al. OCT evaluation of neuroprotective effects of tafluprost on retinal injury after intravitreal injection of endothelin-1 in the rat eye. *Invest Ophthalmol Vis Sci*. 2014;55:1040–1047.
51. Marola OJ, Syc-Mazurek SB, Howell GR, Libby RT. Endothelin 1-induced retinal ganglion cell death is largely mediated by JUN activation. *Cell Death Dis*. 2020;11:811.
52. Kodati B, Stankowska DL, Krishnamoorthy VR, Krishnamoorthy RR. Involvement of c-Jun N-terminal kinase 2 (JNK2) in endothelin-1 (ET-1) mediated neurodegeneration of retinal ganglion cells. *Invest Ophthalmol Vis Sci*. 2021;62:13.
53. Marola OJ, Howell GR, Libby RT. Vascular derived endothelin receptor A controls endothelin-induced retinal ganglion cell death. *Cell Death Discov*. 2022;8:207.
54. Wang X, LeVatte TL, Archibald ML, Chauhan BC. Increase in endothelin B receptor expression in optic nerve astrocytes in endothelin-1 induced chronic experimental optic neuropathy. *Exp Eye Res*. 2009;88:378–385.
55. Marola OJ, Syc-Mazurek SB, Howell GR, Libby RT. Endothelin 1-induced retinal ganglion cell death is largely mediated by JUN activation. *Cell Death Dis*. 2020;11:811.
56. Chaphalkar RM, Stankowska DL, He S, et al. Endothelin-1 mediated decrease in mitochondrial gene expression and bioenergetics contribute to neurodegeneration of retinal ganglion cells. *Sci Rep*. 2020;10:3571.
57. Munemasa Y, Kitaoka Y, Hayashi Y, et al. Effects of unoprostone on phosphorylated extracellular signal-regulated kinase expression in endothelin-1-induced retinal and optic nerve damage. *Vis Neurosci*. 2008;25:197–208.
58. Arfuzir NN, Lambuk L, Jafri AJ, et al. Protective effect of magnesium acetyltaurate against endothelin-induced retinal and optic nerve injury. *Neuroscience*. 2016;325:153–164.
59. Blanco R, Martínez-Navarrete G, Valiente-Soriano FJ, et al. The S1P1 receptor-selective agonist CYM-5442 protects retinal ganglion cells in endothelin-1 induced retinal ganglion cell loss. *Exp Eye Res*. 2017;164:37–45.
60. Nor Arfuzir NN, Agarwal R, Iezhitsa I, Agarwal P, Ismail NM. Magnesium acetyltaurate protects against endothelin-1 induced RGC loss by reducing neuroinflammation in Sprague dawley rats. *Exp Eye Res*. 2020;194:107996.
61. Chen TC, Hoguet A, Junk AK, et al. Spectral-domain OCT: helping the clinician diagnose glaucoma: a report by the American Academy of Ophthalmology. *Ophthalmology*. 2018;125:1817–1827.
62. Geevarghese A, Wollstein G, Ishikawa H, Schuman JS. Optical coherence tomography and glaucoma. *Annu Rev Vis Sci*. 2021;7:693–726.
63. Nagata A, Higashide T, Ohkubo S, Takeda H, Sugiyama K. In vivo quantitative evaluation of the rat retinal nerve fiber layer with optical coherence tomography. *Invest Ophthalmol Vis Sci*. 2009;50:2809–2815.
64. Lakshmanan Y, Wong FSY, Zuo B, Bui BV, Chan HH. Longitudinal outcomes of circumlimbal suture model-induced chronic ocular hypertension in Sprague-Dawley albino rats. *Graefes Arch Clin Exp Ophthalmol*. 2020;258:2715–2728.
65. Lakshmanan Y, Wong FS, Yu WY, et al. Lycium barbarum polysaccharides rescue neurodegeneration in an acute ocular hypertension rat model under pre- and posttreatment conditions. *Invest Ophthalmol Vis Sci*. 2019;60:2023–2033.
66. Hu R, Racette L, Chen KS, Johnson CA. Functional assessment of glaucoma: uncovering progression. *Surv Ophthalmol*. 2020;65:639–661.
67. Prager AJ, Kang JM, Tanna AP. Advances in perimetry for glaucoma. *Curr Opin Ophthalmol*. 2021;32:92–97.
68. Chen RI, Gedde SJ. Assessment of visual field progression in glaucoma. *Curr Opin Ophthalmol*. 2023;34:103–108.
69. Bui BV, Fortune B. Ganglion cell contributions to the rat full-field electroretinogram. *J Physiol*. 2004;555:153–173.
70. Lakshmanan Y, Wong FSY, Zuo B, So K-F, Bui BV, Chan HH-L. Posttreatment intervention with lycium barbarum polysaccharides is neuroprotective in a rat model of chronic ocular hypertension. *Invest Ophthalmol Vis Sci*. 2019;60:4606–4618.
71. Wang Y, Fawzi AA, Varma R, et al. Pilot study of optical coherence tomography measurement of retinal blood flow in retinal and optic nerve diseases. *Invest Ophthalmol Vis Sci*. 2011;52:840–845.
72. Nakazawa T. Ocular blood flow and influencing factors for glaucoma. *Asia Pac J Ophthalmol (Phila)*. 2016;5:38–44.
73. Abe T, Yoshioka T, Song Y, et al. Glaucoma diagnostic performance of retinal blood flow measurement with doppler optical coherence tomography. *Transl Vis Sci Technol*. 2022;11:11.
74. Zhao D, Nguyen CT, Wong VH, et al. Characterization of the circumlimbal suture model of chronic IOP elevation in mice and assessment of changes in gene expression of stretch sensitive channels. *Front Neurosci*. 2017;11:41.
75. Ivanova E, Toychiev AH, Yee CW, Sagdullaev BT. Optimized protocol for retinal wholemount preparation for imaging and immunohistochemistry. *J Vis Exp*. 2013;82:e51018.
76. Cross T, Navarange R, Son J-H, et al. Simple RGC: ImageJ plugins for counting retinal ganglion cells and determining the transduction efficiency of viral vectors in retinal wholemounts. *J Open Res Softw*. 2021;9:15.
77. De Juan JA, Moya FJ, Ripodas A, Bernal R, Fernandez-Cruz A, Fernandez-Durango R. Changes in the density and localisation of endothelin receptors in the early stages of rat diabetic retinopathy and the effect of insulin treatment. *Diabetologia*. 2000;43:773–785.
78. Liu Y, McDowell CM, Zhang Z, Tebow HE, Wordinger RJ, Clark AF. Monitoring retinal morphologic and functional changes in mice following optic nerve crush. *Invest Ophthalmol Vis Sci*. 2014;55:3766–3774.
79. Porciatti V. Electrophysiological assessment of retinal ganglion cell function. *Exp Eye Res*. 2015;141:164–170.